Earth's Future

RESEARCH ARTICLE
10.1029/2022EF002777

The Poverty Impacts of Labor Heat Stress in West Africa Under a Warming Climate

W. Saeed[1], I. Haqiqi[1], Q. Kong[2], M. Huber[2], J. R. Buzan[3,4], S. Chonabayashi[5], K. Motohashi[6], and T. W. Hertel[1]

[1]GTAP, Department of Agricultural Economics, Purdue University, West Lafayette, IN, USA, [2]Department of Earth, Atmospheric and Planetary Sciences, Purdue University, West Lafayette, IN, USA, [3]Department of Climate and Environmental Physics, Physics Institute, University of Bern, Bern, Switzerland, [4]Oeschger Centre for Climate Change Research, University of Bern, Bern, Switzerland, [5]Faculty of Economics, Soka University, Tokyo, Japan, [6]Department of Economics, Tufts University, Medford, MA, USA

Key Points:

- In a global equilibrium economic model analysis, heat-induced labor losses cause significant poverty impacts in West African countries
- Agricultural unskilled labor can see increased wage rates as demands for this type of labor increase in order to dampen food output losses
- Impoverished households' earning sources are key in determining the extent to which a country's poverty headcount is affected

Supporting Information:

Supporting Information may be found in the online version of this article.

Correspondence to:

W. Saeed,
wajihasaeed@gmail.com

Citation:

Saeed, W., Haqiqi, I., Kong, Q., Huber, M., Buzan, J. R., Chonabayashi, S., et al. (2022). The poverty impacts of labor heat stress in West Africa under a warming climate. *Earth's Future*, *10*, e2022EF002777. https://doi.org/10.1029/2022EF002777

Received 14 MAR 2022
Accepted 21 SEP 2022

Author Contributions:

Conceptualization: W. Saeed, I. Haqiqi, M. Huber, T. W. Hertel
Data curation: W. Saeed, I. Haqiqi, Q. Kong, S. Chonabayashi, K. Motohashi
Formal analysis: W. Saeed, Q. Kong, T. W. Hertel
Funding acquisition: T. W. Hertel
Methodology: W. Saeed, I. Haqiqi, Q. Kong, M. Huber, J. R. Buzan, T. W. Hertel
Project Administration: T. W. Hertel

Abstract This paper assesses the poverty implications of heat stress-related labor capacity losses based on simulations using a global general equilibrium economic model. Compared with past studies, we use a more precise measurement of heat stress, assign labor capacity losses to specific labor types by sector, and employ an economic model that contains highly disaggregated economic sectors and regions. This model allows us to determine global and regional economic impacts that account for international dependencies. We focus attention on seven West African countries for which we determine the implied changes in real incomes of households near the poverty line. For these countries, we use household microsimulations to determine potential impacts on the poverty headcount. In our results, poverty impacts are heterogeneous across countries and earning sources-based household strata. A key channel behind this heterogeneity is how loss of labor productivity affects the relative returns to factors of production. We find that unskilled agricultural wages could increase, as loss of productivity in the face of inelastic food demand induces increased labor demand in order to dampen agricultural output losses. In our experiments, even neglecting potential increases in mortality and morbidity, poverty increases range from 2.3% in Cameroon to up to 7.2%–9.2% in Ghana and Nigeria. In one of the seven countries considered, Guinea, poverty sees little change due to the mitigating effects of rising labor wages.

Plain Language Summary With global warming, laborers will experience increasing heat stress and reduced capacity. This will cause economic losses, especially in sectors with high exposure in hot, humid regions. The uneven distributional implications of this, especially on lower-middle income countries, are of special interest. Here, we assess the poverty implications of heat stress on labor globally but with an emphasis on seven West African countries. To estimate poverty impacts in West Africa, we construct global projections of future heat stress and associated labor capacity losses. Surveys of workers provide work intensity and outdoor exposure rates, allowing us to determine which type of workers in which sectors would be affected most. Using a global economic model, we assess the resulting impacts on production, GDP, prices, wages, and incomes. In turn, income changes determine poverty changes. Using recent survey data from seven West African countries, we determine how many households are pushed into poverty under a +3°C global warming scenario. Neglecting potential increases in mortality and morbidity rates, poverty increases in six countries by between 2.3% and 9.2%, while in one country, Guinea, there is little change. In Guinea, agricultural workers can see their wages increase due to increased demand aimed at mitigating food production losses.

1. Introduction

Global warming and subsequent increases in heat stress reduce workers' ability to perform labor in conditions that lack climate control. Many studies suggest that these reductions in labor capacity will be significant (Dunne et al., 2013; Kjellstrom et al., 2009, 2016, 2018; Parsons et al., 2022). Kjellstrom et al. (2018) suggest labor capacity losses in the range of 4%–12%, varying regionally, under 2.7°C mean global warming in a subset of models from the fifth Coupled Model Intercomparison Project (CMIP5) under Representative Concentration Pathway (RCP) 6.0. As workers' capacities are diminished, cascading global economic effects, driven by sectoral and regional interdependencies, result. Recent studies have made important contributions toward assessing the subsequent output and GDP losses across the globe using general equilibrium (GE) methods (de Lima et al., 2021;

Supervision: M. Huber, T. W. Hertel
Writing – review & editing: W. Saeed, I. Haqiqi, Q. Kong, M. Huber, J. R. Buzan, T. W. Hertel

Knittel et al., 2020; Orlov et al., 2020). According to these assessments, the largest GDP declines would occur in Africa and South Asia. These regions comprise low-income economies that are home to a large share of the world's present-day poor, which raises questions as to the extent to which international poverty reduction goals could face significant headwinds due to this aspect of climate change. It has been proposed that heat stress is a great driver of inequality since it harms those most vulnerable (Alizadeh et al., 2022; Rogers et al., 2021) and this is further supported and quantified in our study.

In this paper, we assess the poverty implications of heat stress-induced labor capacity losses in seven West African countries: Ghana, Burkina Faso, Cameroon, Cote d'Ivoire, Guinea, Nigeria, and Senegal. The focus of this paper is on the potential for heat stress-induced labor capacity losses to increase poverty rates and the economic channels that would drive these increases. We focus on the West African region, given that existing poverty rates in the region are among the highest in the world, and levels of national income (e.g., as measured by GDP per capita) are among the lowest. Arguably, this makes the region among the least capable of responding to heat stress with capital intensification.

We use a global GE macroeconomic model to assess economic impacts, including expected changes in prices of commodities and returns to factors of production globally. More specifically, within such a model, we simulate the labor productivity losses of heat stress consistent with a 3°C warmer world, where the estimated changes in labor capacity account for heterogeneities across labor types, sectors, and countries. By using a GE approach, we account for the complete circular flow of income and of goods and services within countries as well as globally. This is important, since impacts in one sector produce ripple effects flowing into other sectors through input-output relationships as well as competition for labor and other resources. Second, we account for regional dependencies and changing comparative advantage, which are important to consider when assessing global climate change impacts. In this regard, West Africa is not alone in experiencing increases in heat stress. While any given country may suffer economic consequences from increased heat stress within its borders, it will also be affected through changing world prices induced by developments in other countries. The economic impacts reported in this analysis account for such interlinkages.

The changes in prices of commodities and factors of production assessed using this GE approach are then used as inputs into a household microsimulation exercise for each of the seven countries using the latest available household income survey data. In this way, we assess how significantly the poverty headcount is affected, within this experimental setting, across these different countries that vary in economic structure and in the number and composition of poor households. We also explore how poverty impacts vary across different household types within each country. (Present-day poverty rates within and across these seven countries are provided in Table S1 and Figure S1 in Supporting Information S1).

Given this ultimate objective, a static GE model has been employed. That is, we do not examine the path of adjustment from the current economy to a future economy burdened by climate change, only the final outcome. We simulate the effects of projected future heat stress on the present-day economy and examine the final outcome. This approach of imposing a future scenario on the present-day economy (similar to that used by de Lima et al., 2021 and Hertel et al., 2010) has the advantage of allowing us to decompose observed outcomes to reveal which factors and economic features would drive changes in poverty when labor is affected by heat stress. We recognize that the composition of poverty, as well as sources of earnings and spending patterns, will change in the future, but there is no established methodology for predicting these changes at the level of individual households. Therefore, our estimates should not be construed as forecasts of future poverty rates, rather we seek to highlight the mechanisms through which a warming climate will likely affect the poorest households in West Africa.

We find that poverty impacts are heterogeneous in size across countries in our experiment and that it is possible for some households to be unexpected monetary beneficiaries from climate-induced heat stress. Therefore, to gain a better understanding of the mechanisms and household features that drive country-level poverty changes and how benefits can also theoretically arise, we highlight the impacts in the largest country in terms of population, Nigeria, where we fully decompose the drivers of poverty changes.

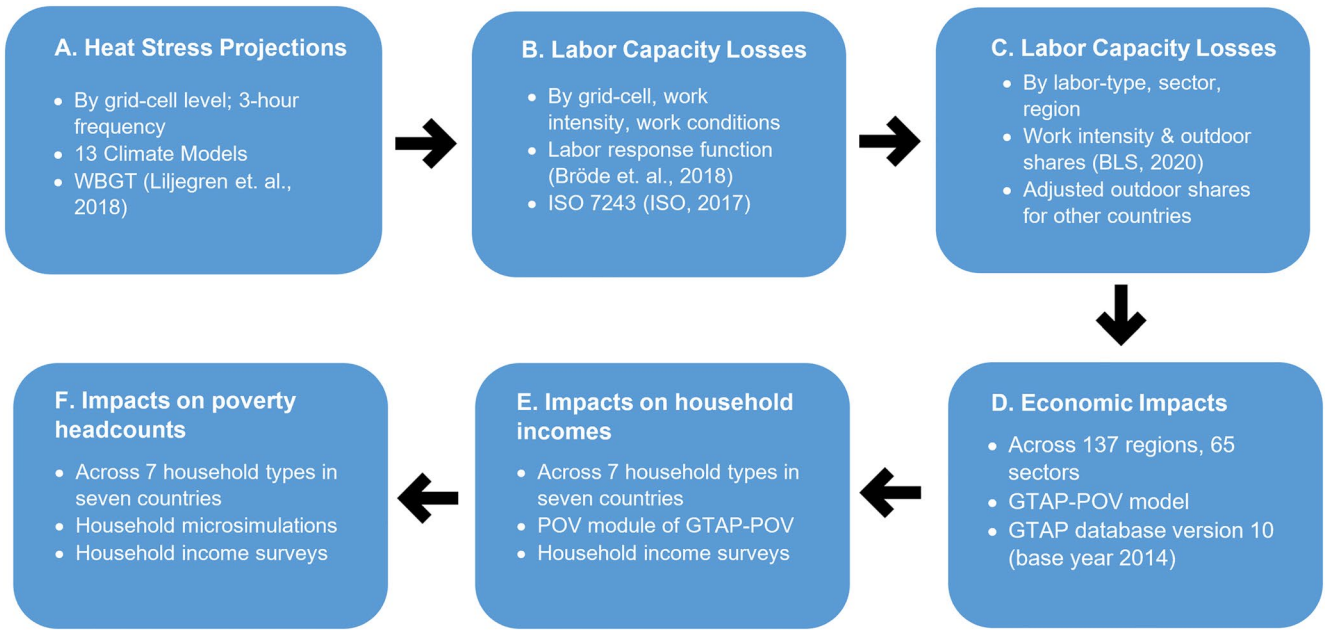

Figure 1. Overview of methods and data used.

2. Materials and Methods

2.1. Overview of Methods

To assess the poverty implications of heat stress-induced labor capacity losses, this paper broadly follows a path similar to that of the recent economic assessments (de Lima et al., 2021; Knittel et al., 2020; Orlov et al., 2020). This entails the following major steps: (A) We first quantify heat stress intensification by comparing a baseline period (1961–1990) with a 3°C global mean warming scenario. Heat stress is measured by the Wet Bulb Globe Temperature (WBGT) using Liljegren et al. (2008)'s formulation, which as described in Kong and Huber (2022) avoids the ad hoc approximations used in prior studies (de Lima et al., 2021; Knittel et al., 2020; Orlov et al., 2020). (B) The resulting labor capacity losses are then determined using a labor response function. In this paper, we apply the ISO Standard 7243 (ISO, 2017) using the approach of Bröde et al. (2018). ISO 7243 is an international standard providing guidance on the assessment and control of hot environments based on WBGT (ISO, 2017). This assumes that workplace safety standards designed to prevent increases in mortality and morbidities are followed. In a sensitivity analysis, we also consider economic impacts when an alternative labor response function based on empirical measurements of labor productivities under heat is employed. (C) These labor capacity losses are then used as inputs into a global GE economic model, dubbed GTAP-POV (Hertel et al., 2011). (D) The central innovation in this paper, in addition to the more accurate WBGT formulation, is the assessment of impacts on impoverished households, as well as the overall poverty headcount. We assess these using price and wage changes determined by the main global GE model as inputs into a microsimulation module (described in later sections) that permits us to make inferences about changes in the poverty headcount nationally as well as by type of household. These steps—the broad methods and key data sources used—are summarized in Figure 1 while more detailed descriptions are provided in the sections that follow.

While the primary objective and innovation of this study are the assessment of poverty impacts, the methods used in steps (A–C) extend those used in prior studies in several ways. First, in step (A), we use a more accurate approach to calculate WBGT. Second, for step (C), we use an improved approach to assign labor capacity losses (under different work intensities and indoor/outdoor conditions) to specific economic sectors and labor types. We also use an economic model with far greater detail that allows us to assess economic impacts at the level of 137 individual countries/regions and 65 sectors. This study therefore also serves to provide new, more refined assessments of the global economic impacts of human heat stress from climate change.

2.2. Estimation of Heat Stress

As mentioned, in this study, heat stress is measured by WBGT, which is a widely used heat stress metric incorporating the effects of all four ambient factors (temperature, humidity, wind, and radiation). It has well-established safety thresholds within the athletic (American College of Sports Medicine, 1984), occupational (Coco et al., 2016), and military settings (Sawka et al., 2003). However, WBGT is not available as a routine meteorological measurement, and various approaches have been developed to approximate it. The simplified WBGT (ABM, 2010) and environment stress index (Moran et al., 2001, 2003) represent two relatively simple ad hoc approximations. However, these are subject to potentially large biases when used out of the conditions under which they were developed (Grundstein & Cooper, 2018; Havenith & Fiala, 2011; Kong & Huber, 2022). As demonstrated recently in Kong and Huber (2022), use of simplified WBGT leads to large and systematic overestimates of labor capacity reductions which materially impacts the interpretations of prior work using that metric (Altinsoy & Yildirim, 2015; Chavaillaz et al., 2019; de Lima et al., 2021; Lee & Min, 2018; Liu, 2020; Matsumoto et al., 2021; Zhang & Shindell, 2021; Zhu et al., 2021).Instead, we use a physically based model developed by Liljegren et al. (2008) to directly simulate WBGT measurements, which is expected to render more accurate WBGT estimates than past studies.

Liljegren's model has been extensively calibrated and validated (with an RMS difference of less than 1°C) and has seen increasing applications in recent years (Casanueva et al., 2020; Takakura et al., 2017). Kong and Huber (2022) developed a Python implementation of Liljegren's code (originally in FORTRAN and C language), which is especially suitable for processing large-size climate model output and is adopted in this paper. For the detailed calculation procedure of WBGT, see Liljegren et al. (2008) and Kong and Huber (2022).

2.3. Heat Stress Projection

Heat stress intensification is quantified by focusing on a 3°C warming of global mean surface air temperature compared to the baseline period 1961–1990, which corresponds to a near upper-bound projection of global warming by the end of this century based on recent estimates of possible emission pathways (Moore et al., 2022). The CMIP6 historical and SSP585 scenarios are adopted for heat stress evaluation under baseline and 3°C warming, respectively. To locate the period corresponding to a 3°C warming, we index each year in SSP585 simulations by the degree of warming (compared with the baseline period) and select years falling into a range of 2.75–3.25°C warming which are then used to represent a 3°C warming world.

However, our results are not sensitive to the driving scenario since the GCM results are scaled to specific warming levels and these responses are robust (Buzan & Huber, 2020). This approach is becoming common in climate change impact studies (e.g., Parsons et al., 2021; Schwingshackl et al., 2021). By focusing on labor loss at a certain warming target, we decouple our analysis from the time path of forcing, thereby reducing uncertainties caused by model spread due to climate sensitivity. This removes issues related to "when does warming happen" and "what scenario of emissions is being followed." In addition, bias correction is conducted by adding WBGT anomalies from CMIP6 climate models onto a common ERA5 reanalysis baseline (1961–1990) (Hersbach et al., 2018). For model details of bias correction procedure, please refer to Text S1 in Supporting Information S1.

2.4. Estimation of Labor Capacity Losses

Next, the projections of heat stress/WBGT are translated into projections of labor capacity losses. Multiple labor response functions (LRFs) have been proposed for this purpose (Bröde et al., 2018; Dunne et al., 2013; Foster et al., 2021; ISO, 2017; Kjellstrom et al., 2018). However, largely different estimates of heat stress-induced labor loss are generated by these LRFs. Here, we use two LRFs, namely the one based on ISO7243 standard (ISO-LRF) (Bröde et al., 2018; ISO, 2017) and the one adopted in recent reports of the Lancet Countdown on health and climate change (Lancet-LRF) (Romanello et al., 2021; Watts et al., 2021), which is based on the work of Kjellstrom et al. (2018). By adopting two LRFs, we provide an assessment of the uncertainty stemming from assumptions on the functional relationship between heat stress and labor performance. The two chosen approaches are the most widely adopted and represent very different philosophies in quantifying heat impact on labor. ISO-LRF was designed to prevent heat injury by implementing work-rest cycles and is designed to avoid health risk; Lancet-LRF is based on a statistical fitting on labor productivity measurements within observed workplaces (Kjellstrom et al., 2018; Sahu et al., 2013; Wyndham, 1969) and thus is less restrictive but also more

likely to be associated with the adverse health impacts that are amply evidenced (Flouris et al., 2018; Romanello et al., 2021). An excellent discussion of the relative merits of these two different approaches is included within Ioannou et al., 2022 and we will not recapitulate it here. A comparison of labor capacities as a function of WBGT as predicted by both LRFs is demonstrated in Figure S2 in Supporting Information S1.

ISO-LRF starts with $WBGT_{lim}$ corresponding to the upper limit of the prescriptive zone. Workers are recommended to work for only a fraction of each hour when the environment WBGT values exceed this reference value. $WBGT_{lim}$ can be calculated by the equation below which is adopted by both the ISO 7243 (INS, 2017) and NIOSH (Coco et al., 2016):

$$WBGT_{\text{lim}} = 56.7 - 11.5\log_{10}(M) \tag{1}$$

where M refers to metabolic heat production rates in Watts. Labor capacity can be then obtained by the following equation:

$$Labor\ Capacity = \max\left\{0, \min\left[1; \frac{WBGT_{\text{lim},rest} - WBGT}{WBGT_{\text{lim},rest} - WBGT_{\text{lim}}}\right]\right\} \tag{2}$$

where $WBGT_{lim,rest}$ refers to the limit WBGT value when people are at rest ($M = 117W$).

Lancet-LRF follows the "hothap" LRF developed by Kjellstrom et al. (2018) except without the cutoff at 10% and 90% of labor productivity (Romanello et al., 2021; Watts et al., 2021):

$$Labor\ Loss\ Fraction = \frac{1}{2}\left[1 + erf\left(\frac{WBGT - \mu}{\sigma\sqrt{2}}\right)\right] \tag{3}$$

where erf is a cumulative normal distribution function; μ and σ denote the mean and standard deviation of the associated normal distribution and are tabulated in Table S2 in Supporting Information S1 for different levels of working intensity.

In implementing the LRFs as described above, assumptions must be made with regards to the intensity of physical activity, the conditions under which this activity takes place: Outdoors or indoors (shaded, without air-conditioning) and the working profile. In this study, we estimate, for each grid cell, labor capacity declines for four different levels of work intensity ranging from light to very heavy work (metabolic outputs of 200, 300, and 400W). Each of these is estimated under both indoor without air-conditioning and outdoor conditions. Since people mostly work during the daytime (especially in heavily affected sectors such as agriculture and construction), the calculation only includes daytime hours. We recognize that night-shifting has been proposed as a potential adaptation strategy to increasing heat stress (Takakura et al., 2018). However, there exist large uncertainties regarding when and to what extent night-shifting can be implemented. Therefore, this is not considered in this study in keeping with other similar studies (Watts et al., 2021). The percentage decline in labor capacity under 3°C warming is estimated relative to baseline period labor capacity.

In past studies, simplistic assumptions were used to assign these labor capacity losses to economic sectors, such as assuming all agricultural labor is done at a single work intensity and entirely indoors or outdoors. For our analysis, rather than apply one intensity-exposure profile to each sector, we use data from the US Bureau of Labor Statistics (BLS, 2020) to assign weights to these different estimates and produce labor capacity losses that apply to specific labor types within specific sectors and countries. The BLS data identify the types of workers employed in different sectors and provide descriptors regarding their intensity of work (ranging from "sedentary" to "very heavy") and their exposure to the outdoors (ranging from "never" to "constant"). We map these descriptors to specific assumptions about metabolic output (e.g., we assume "heavy" to "very heavy work" is equivalent to metabolic output of 400W). These assumptions are described further in Text S2 in Supporting Information S1.

Formally, we estimate using the following equation:

$$z_{l,a,r,g} = \sum_{c}\sum_{i} z_{r,g}^{i,c}\alpha_{l,a}^{c}\beta_{l,a}^{i} \tag{4}$$

where $z_{l.a.r.g}$ is the labor capacity loss of labor type l in activity a in grid cell g of region r. These sector specific labor capacity losses are obtained by weighting $z_{r.g}^{i,c}$: The percentage decline in labor capacity in grid cell g (in

region r), for work performed at intensity i where $i = \{200W, 300W, 400W, 600W\}$, and in indoor or outdoor conditions indicated by the index c where $c = \{\text{indoors}, \text{outdoors}\}$, under heat stress levels consistent with 3°C mean global warming. The weights in question are $\alpha^c_{l,a}$, the portion of time that labor type l in activity a is exposed to work conditions c and $\beta^i_{l,a}$, the portion of work of labor type l in activity a that is performed at work intensity i.

The BLS data are, however, specific to the U.S. economy and the shares $\alpha^c_{l,a}$ that measure exposure to outdoor work of different labor types in different sectors could be a poor approximation of work conditions in low-income countries. This is especially true for agricultural workers whose exposure to the outdoors is likely to be far more frequent in low-income countries than in the United States. We therefore adjust the shares of outdoor work by assuming that these decline with a country's GDP per capita. This captures approximately the higher rates of mechanization and other technological improvements in higher income economies that may allow labor to be less exposed to outdoor conditions. More specifically, we assume that there exists an exponential decay relationship that relates outdoor work share and GDP per capita. The specific assumptions made in order to perform this adjustment of outdoor labor shares are described within Text S2 in Supporting Information S1, along with alternatives considered, and the sensitivity of our results to this assumption regarding functional form is shown in Figures S5 and S6 in Supporting Information S1.

Finally, we aggregate the grid-level labor capacity losses ($z_{l,a,g,r}$) over grid cells to obtain region, sector, and labor specific capacity losses ($z_{l,a,r}$). To do so, grid cells are weighted by their population when aggregating labor capacity losses for nonagricultural activities and by their share in national agricultural production when aggregating labor capacity losses for agricultural activities. Further details are provided in Text S3 in Supporting Information S1.

2.5. Economic Framework

2.5.1. Overview of Economic Approach

As described in the previous section, we determine labor capacity losses that are specific to countries, labor types, and sectors. These losses are treated as labor productivity shocks in a global GE economic model, GTAP. However, given the importance of labor markets to our findings, we depart from the standard GTAP model assumption of perfect labor mobility across sectors. We do this by incorporating elements of GTAP-AGR (Keeney & Hertel, 2005) that allow for labor market segmentation such that workers are imperfectly mobile across agricultural and nonagricultural sectors, resulting in wage differentials between these sectors.

For the estimation of poverty impacts, we use elements of GTAP-POV (Hertel et al., 2011), an extended version of the standard GTAP model (Corong et al., 2017; Hertel, 1997). The -POV extension to GTAP estimates changes in the real incomes of households near the poverty line, and the resulting poverty changes using an elasticity approach. However, we deviate from the standard GTAP-POV elasticity approach and, for greater precision, instead use a household microsimulation that is described in the next section.

The underlying economic database of the global economic model is version 10 of the GTAP database (Aguiar et al., 2019), which has a base year of 2014. As noted earlier, the analysis undertaken here is comparative static such that we impose labor capacity losses associated with a future climate (one of 3°C mean global warming) on the present-day economy. This allows us to identify the mechanisms that drive our results with relative clarity and avoid uncertainties associated with projecting what the global economy—as well as patterns of poverty and household earnings—might look like in a distant future (when an outcome such as 3°C mean global warming might come to pass). In order to assess poverty impacts, such a projection would require us to somehow estimate who will be poor in the future, where they live, how they earn their income, and so on. Taking this approach would introduce enormous uncertainties and make results difficult to interpret since they would be driven by a combination of economic mechanisms and the assumptions made to achieve a projection of the future economy. By taking a comparative static approach, this complication is avoided and the economic mechanisms at play are easier to identify.

2.5.2. Estimation of Poverty Impacts

Changes in poverty are estimated using a household microsimulation approach as follows. The GTAP global economic model determines economic impacts that include changes in the prices of consumption goods and

Table 1
Definitions of Household Strata

No.	Stratum name (short name)	Description
1	Agricultural Households (AGRICULT)	Households that earn more than 95% of their income from agricultural self-employment.
2	Nonagricultural households (NNAGRICULT)	Households that earn 95% of their income from non-agricultural self-employment.
3	Urban Labor households (URBLABOR)	Households located in urban areas that earn 95% of their income from wage labor.
4	Rural Labor households (RURLABOR)	Households located in rural areas that earn 95% of their income from wage labor.
5	Transfer Income households (TRANSFER)	Households that earn 95% of their income from transfers.
6	Urban Diverse households (URBDIVRS)	Urban households that do not fall under any other category.
7	Rural Diverse households (RURDIVRS)	Rural households that do not fall under any other category.

factors of production. In turn, these price changes are used as inputs to estimate how real incomes of households close to the poverty line change, using the GTAP-POV extension. Finally, changes in real income are used to estimate changes in poverty using a microsimulation approach. This last step departs from the standard GTAP-POV approach that estimates poverty impacts using an elasticity approach, which can be seen as an approximation of the microsimulation approach adopted here. Key elements of these steps are summarized as follows, while a detailed exposition of GTAP-POV is provided in Hertel et al. (2011).

For each country included in the poverty module, we employ household survey data to identify households that are "in the neighborhood of the poverty line." This is defined as the decile of households that encompass the $1.90-per-day international poverty line as defined by the World Bank (Ferreira et al., 2016). These households are then classified into seven strata based on how they earn their income. For example, households are classified as "agricultural" if they earn 95% or more of their income from agricultural self-employment and as "urban labor" if they reside in urban areas and earn 95% or more of their income from wages. If households are not specialized, such that they do not earn 95% or more of their income from either self-employment or wages, then they are classified as rural or urban diverse (See Table 1 for definitions of all seven strata).

In this way, the module takes into account the heterogeneity in how the poor earn their income. As we will see below, this is an important factor in assessing the poverty impacts of human heat stress. Next, the specific profile of households within each stratum in terms of earning shares is determined. For example, for households in the agricultural stratum in each country, we determine the share of their income they earn from land, capital, unskilled agricultural labor, unskilled wage labor, etc. The real income of households within each stratum (within each country of focus) depends on these earning shares, and for our analysis we must also account for the loss of earnings from labor due to the direct effect of heat stress-induced productivity loss. Formally, we determine the percentage change in the real income of households in a stratum s (in region r) as follows:

$$\hat{y}_{r,s} = \sum_i \alpha_{r,s,j} \left(\hat{W}_{r,j} - \hat{Z}_{r,j} - \hat{C}_r \right) \tag{5}$$

where $\alpha_{r,s,i}$ are the aforementioned earnings' shares, that is, $\alpha_{r,s,i}$ is the share of income of households in stratum s in region r earned from factor i. $\hat{W}_{r,i}$ is the percentage change in the price of (returns to) factor i determined from the main macro model, and $\hat{Z}_{r,i}$ is the loss of productivity of factor i reflecting diminished working hours. Earnings are also adjusted by $\hat{C}_r$, the change in the real cost of living of households at the poverty line given changes in consumption prices and consumption patterns of poor households in region r.

Given these changes in the real incomes of households, we determine changes in the poverty headcount using a microsimulation approach. This approach is used in place of the elasticity approach that is implemented in the GTAP-POV model. The household microsimulation approach is more direct and exhaustive: We consider each individual household in the neighborhood of poverty; shock its income by the size of $\hat{y}_{r,s}$; and count the number

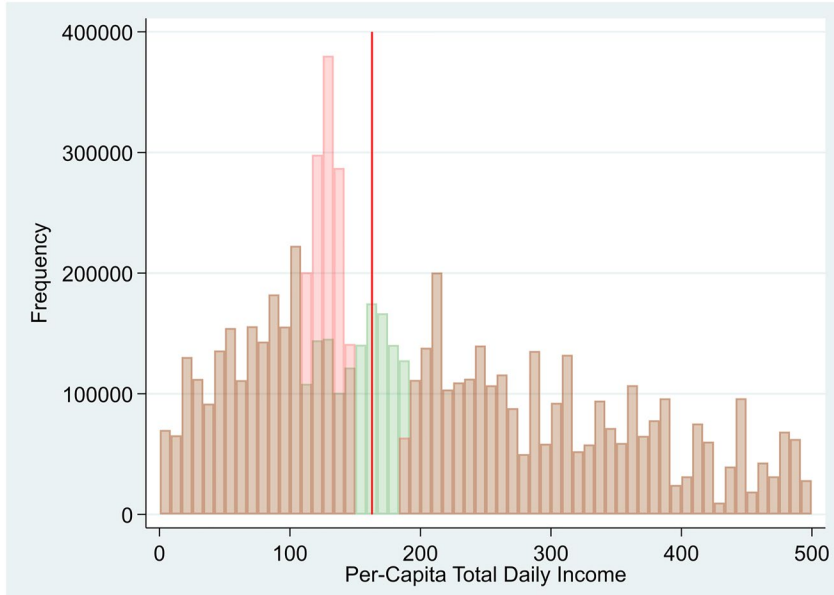

Figure 2. Household microsimulation for Nigeria's rural diverse households. Notes: Figure uses data from Nigeria's General Household Survey, 2018 (NBS, 2018). Only households with per capita incomes less than ₦500 are shown. Red vertical line indicates the poverty line in terms of Nigerian Naira consistent with a 39.1% poverty rate as reported by the World Bank's World Development Indicators for the year 2018 based on the $1.90 per day international poverty line. Green bars show the original ex ante survey-based income distribution of households. Red bars show the ex post distribution of households after implementing income shock estimated using Equation 5.

of households whose incomes fall below the poverty line. This has the advantage that it uses individual observations in the household survey, thereby utilizing the actual distribution of household observations as opposed to summarizing the distribution in a single elasticity metric.

The microsimulation approach is illustrated for the case of Nigeria's rural diverse stratum in Figure 2 below. It shows the distribution of rural diverse households around the poverty line, and how this distribution shifts when the incomes of households in the "neighborhood of poverty" fall by the relevant $\hat{y}_{rs}$. As will be detailed in the results sections, this approach suggests a 15.8% increase in poverty among rural diverse households in Nigeria.

This exercise must be done individually for all households in each country for which poverty impacts are to be assessed. It is for this reason that our analysis of poverty is limited to seven countries for which the necessary household survey data are available and have been stratified and processed in the manner required for this modeling framework.

2.6. Data

The specific data sources used at each step of this study are detailed as follows:

2.6.1. Climate Data

CMIP6 data were retrieved at 3-hourly frequency to estimate WBGT using the Liljegren approach. A sample of 10 climate models (13 ensemble members) are included which represent all models with all necessary input variables archived at the required temporal resolution. The models and ensemble members used are listed in Table S4 in Supporting Information S1. The retrieved inputs include 2m air temperature, surface specific humidity, surface pressure, 10m wind, and surface downward and upwelling components of both short- and long-wave radiation. WBGT is calculated under both outdoor and indoor conditions. For indoor conditions, solar radiation is set to zero and wind speed is fixed at 1 m/s, a typical value for air speed relative to an indoor laborer.

2.6.2. BLS Data

To estimate labor capacity losses specific to labor types and economic sectors within each region, we estimate indoor/outdoor exposure and work intensity shares ($\alpha's$ and $\beta's$ in Equation 3) using data from the Occupational Requirements Survey 2020 from the U.S. Bureau of Labor Statistics (BLS, 2020). These are described in Text S2 in Supporting Information S1.

2.6.3. World Gridded Population Data

To calculate the country-level weighted average of capacity losses for nonagricultural activities, we use the Gridded Population of the World (CIESIN, 2018) for the year 2010. The data are aggregated from the 5 arcmin original resolution to the climate data resolution (30 arcmin and 60 arcmin). Here, we assume the spatial distribution pattern of the population stays the same. Note that this information is used for calculating a spatially weighted average, thus while the pattern is important, the total population has no impact on the final calculation. The country and regional boundaries for aggregation are obtained from Baldos (2017).

2.6.4. World Gridded Agricultural Production Data

To calculate the country-level weighted average of capacity losses for agricultural activities, we calculate the gridded value of agricultural production following the method used in the SIMPLE-G data set (Baldos et al., 2020; Haqiqi et al., 2020). The value of production is calculated based on the gridded information about harvested area by crop, yield by crop, and the average national price of crops. The harvested area and yields are obtained from Global Crop Water Model outputs (Siebert & Döll, 2010) combined with country-level information on prices from FAO (FAO, 2020).

2.6.5. GTAP Database

In our implementation of the GTAP-POV model, we use version 10 of the GTAP database (Aguiar et al., 2019). For the implementation of the -POV module, see GTAP-POV technical paper (Hertel et al., 2011).

2.6.6. Household Income Survey Data Sets

For the seven West African countries of focus, the household survey data sets used are as follows: Ghana Living Standard Survey 2017 (GSS, 2018), Burkina Faso 2014 (INSD, 2014), Fourth Cameroon Household Survey 2014 (INS, 2017), Cote d'Ivoire Household Standard of Living Survey 2015 (INS-CI, 2015), Guinea Poverty Assessment Survey 2012 (INS-Guinée, 2012), Nigeria General Household Survey 2018 (NBS, 2018), and Senegal Poverty Monitoring Survey 2015 (ANSD, 2011).

2.6.7. Poverty Data

Poverty headcount ratio at $1.90 a day (2011 PPP) (% of population) was obtained from the World Bank World Development Indicators database (https://databank.worldbank.org/source/world-development-indicators) retrieved in December 2021.

Thus, our results are based on the underlying assumption that the "present-day" economy is broadly reflected by economic conditions of 2014 and population distribution (at the grid-cell level) of 2010 (which are used in order to aggregate grid-cell level capacity losses in order to obtain country-level estimates). In the case of poverty data, we sought the latest available information regarding the levels and distribution of poverty in each of our countries of interest. While these underlying data relate to different years, we believe the mismatch is not of great significance for our objectives of delineating the mechanisms that drive poverty impacts. Furthermore, broad economic structures (as captured by the GTAP database in our case) do not change rapidly from year to year. Hence, the advantages of seeking economic, population, and poverty data from a single year (likely an impossible task) would be minimal.

10.1029/2022EF002777

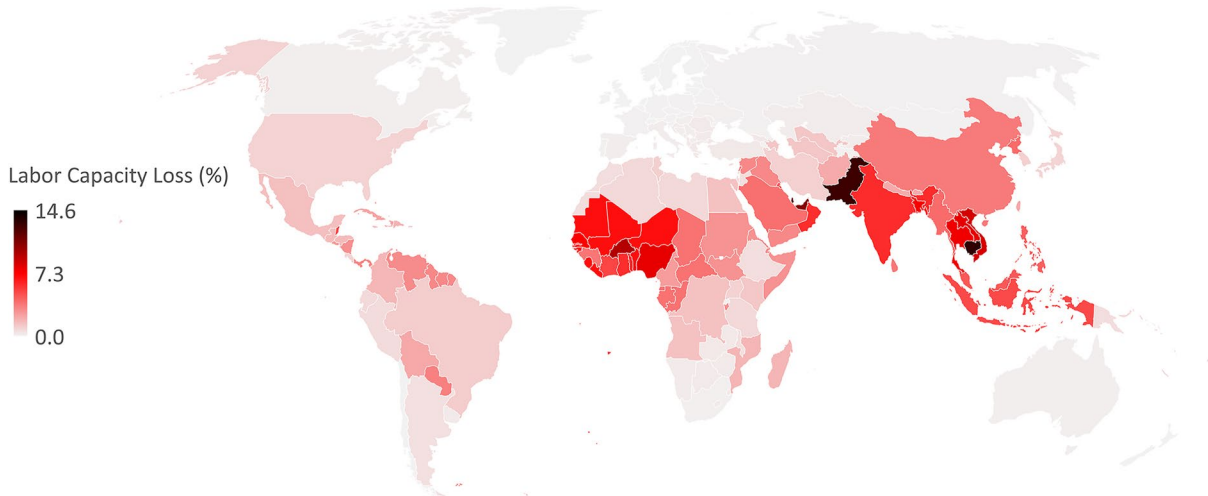

Figure 3. Country-level labor capacity losses. Note: Labor capacity losses are relative to 1961–1990. Country-level labor capacity losses are constructed as weighted average of labor capacity losses across all 65 sectors and four labor types using employment shares from GTAP database version 10 as weights.

Also note that throughout this paper, we refer to 3°C warming relative to the base period 1961–1990. Relative to 2010–2020, this is approximately equivalent to 2.3°C of warming.

3. Results

3.1. Labor Capacity and GDP Losses

Given the various methodological improvements that have been made over past studies in estimating labor capacity losses, we begin with briefly reporting our estimates of the projected labor reduction relative to the 1961–1990 baseline across the globe to allow for comparison with previous estimates. In terms of broad aggregates, our results are consistent with past studies (ILO, 2019; Orlov et al., 2020; Parsons et al., 2021): The largest labor capacity losses are in South Asia and parts of the Middle East followed by Southeast Asia and West Africa (Figure 3). We find that the worst affected countries are (in descending order, starting from most affected) Bahrain, Cambodia, Pakistan, Qatar, and the UAE which lose 11%–15% of their annual labor capacity relative to the baseline.

However, GDP losses (Figure 4) are most pronounced in West Africa. Across the seven countries of focus, labor capacity losses range from 5% to 9.4% while their GDP losses constitute some of the largest GDP losses across the 139 countries/regions in our model (See Table S5 in Supporting Information S1). Nigeria, in particular, suffers the largest annual GDP decline in the world (tied with Cambodia), exceeding 5% in our experiments. The

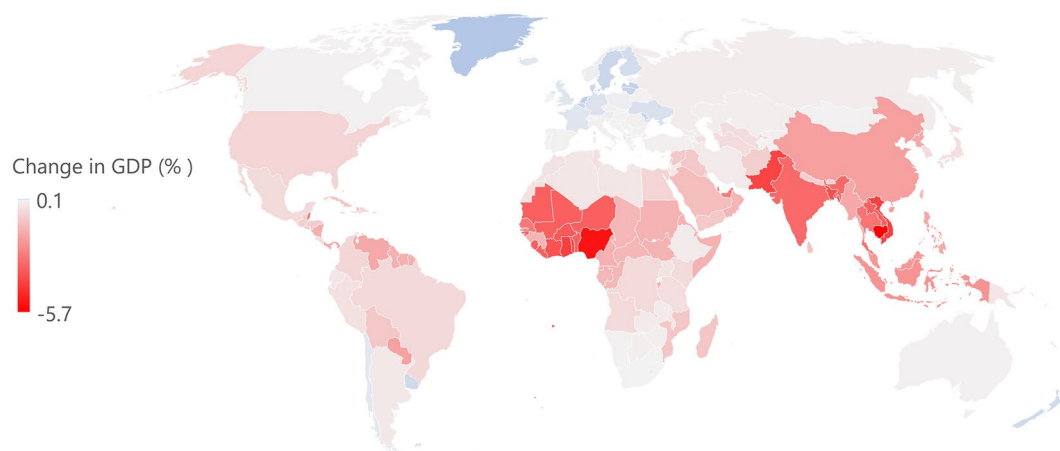

Figure 4. Country-level GDP losses.

10.1029/2022EF002777

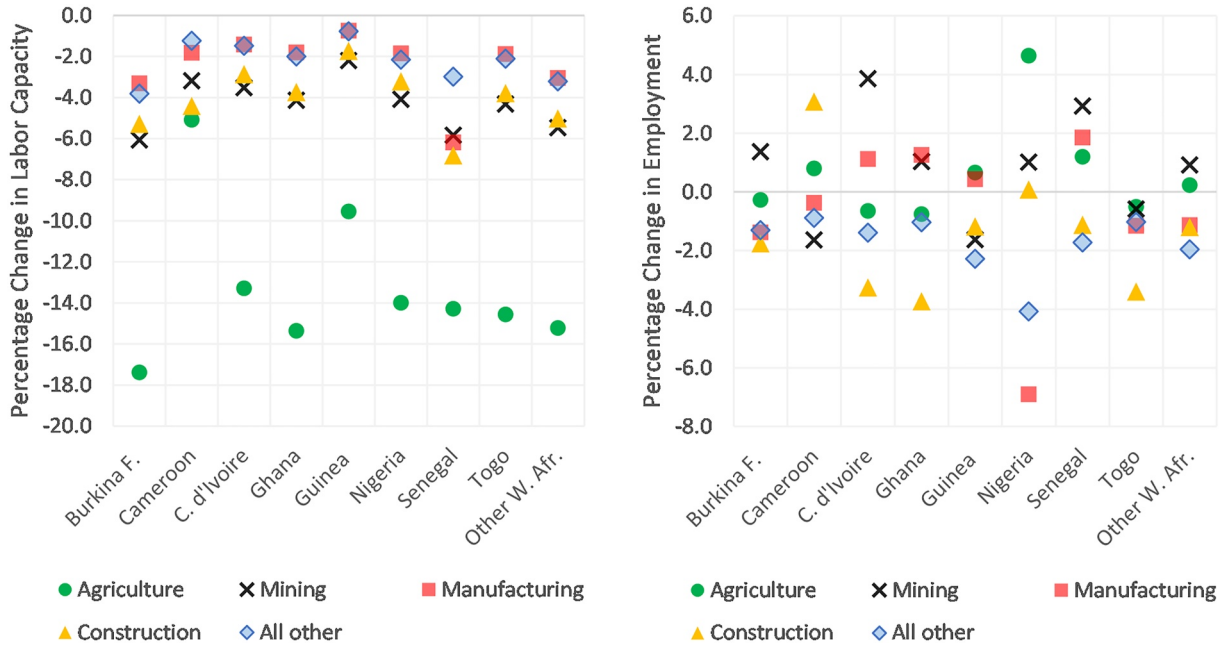

Figure 5. Labor capacity losses (left panel) and change in employment (right panel) by region and aggregate sectors in West Africa. Note: Figure shows labor capacity and employment changes by region and aggregated sector by averaging over labor types and subsectors using employment in the base as weights. Labor capacity losses are relative to 1961–1990. The mapping from the 65 GTAP sectors to the five aggregate sectors shown is reported in Table S7 in Supporting Information S1.

remaining six West African countries of focus experience GDP losses ranging from 2.9% (in Senegal) to 4.3% (in Ghana). The more pronounced GDP losses in West Africa stem from the relatively greater dependence on agriculture and high levels of unskilled labor concentrated in agriculture. These features lend further support to our focus on this region for the ensuing poverty assessments.

As detailed in the methods section, these results are based on the ISO-LRF approach to measuring labor capacity losses. As such, they should be interpreted as the economic costs of averting loss of life and adverse health outcomes. Using the alternative, empirically determined Lancet-LRF, labor capacity and GDP losses are predictably smaller since workplace safety standards are not necessarily followed and hence workers work more than the recommended amount. Under the Lancet-LRF approach, in the seven West African countries labor losses range from 2.2% to 5.2%. That is, in these seven countries, country-level labor capacity losses are on average 44% smaller than the ISO-LRF approach. (See Figure S7 in Supporting Information S1). The resulting GDP losses are similarly smaller as are country-level poverty increases (see Figure S8 in Supporting Information S1). However, these losses do not factor in the adverse health outcomes that will inevitably follow from the failure to provide workers with sufficient rest times and this approach therefore provides an incomplete assessment of the long run impacts of human heat stress on the economy and poverty. It is for this reason that we focus on ISO-based results.

3.2. Sectoral Drivers of Labor Capacity Losses in West Africa

Country-level aggregate results such as those shown in the preceding section can mask disparities across sectors within a country. A sectorally disaggregated view of labor capacity losses in West Africa is provided in Figure 5. It shows that in terms of broadly defined sectors, agriculture is generally the most affected and will suffer especially large capacity losses in West African countries. Among the seven countries of focus, the single largest percentage reduction in labor capacity, of 17.4%, occurs in Burkina Faso's agricultural sector. Agriculture activity in the other West African countries sees labor capacity losses ranging between 9% and 16%. Cameroon is the exception in our subsample where agriculture sees a relatively smaller 5% labor capacity loss. After agriculture, the construction and mining sectors tend to be the most affected; however, labor capacity losses in these sectors rarely exceed 6% in West Africa.

10.1029/2022EF002777

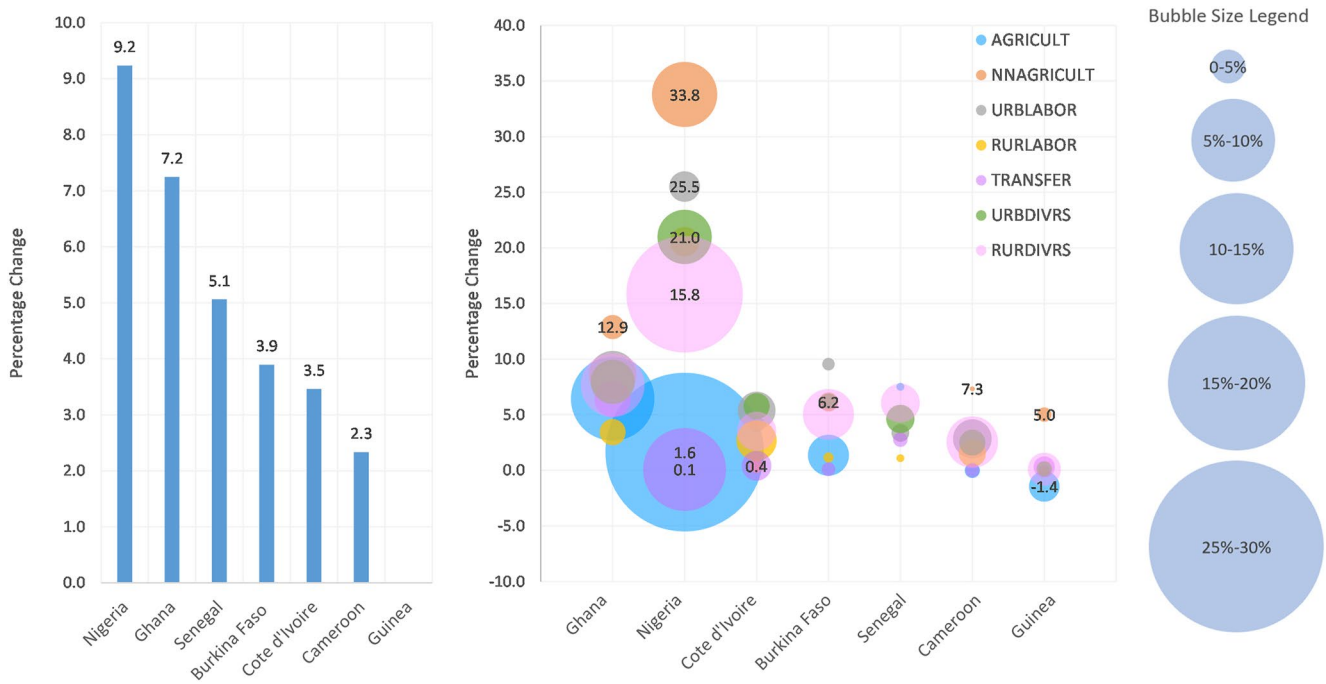

Figure 6. Changes in the poverty headcount (percentage change), by country (left) and by country and strata (right). Notes: Bubbles in right panel represent strata where location of midpoint/center of bubble on the *y*-axis shows percentage change in poverty for the stratum (e.g., the nonagricultural stratum in Nigeria sees a poverty increase of 33.8% as shown by the data label in some illustrative cases); and size of bubble is proportionate to the stratum's percentage share in baseline poverty levels in West Africa (e.g., the agricultural stratum of Nigeria accounts for 25% of West Africa's poverty in the base). Negative poverty changes occur only in Guinea. Thus, higher and larger bubbles represent strata that are larger contributors to overall poverty increases in West Africa. Household strata are defined as follows. AGRICULT: households that earn more than 95% of their income from agricultural self-employment; NNAGRICULT: households that earn 95% of their income from nonagricultural self-employment; URBLABOR: urban households that earn 95% of their income from wage labor; RURLABOR: rural households that earn 95% of their income from wage labor; TRANSFER: households that earn 95% of their income from transfers; and URBDIVRS and RURDIVRS: urban and rural households that do not fall under any other category.

Furthermore, in addition to loss of labor capacity, some sectors can lose workers in the face of price-induced market responses, while others can see labor employment increase in order to partially mitigate the effects of the labor capacity losses. Across the seven West African countries of focus, employment shifts across sectors are mixed (see Figure 5b). For example, in Ghana labor productivity losses in agriculture are compounded further by the loss of labor to other sectors; but the reverse is true in Nigeria where labor is drawn into agriculture due to the strong increase in food prices and farm wages. This ambiguity in employment outcomes across regions highlights the role of competing economic forces: On the one hand, loss of labor productivity warrants an increase in labor numbers to compensate for lost productivity; on the other hand, there are pressures to cede labor to competing sectors where labor can be more valuable.

The results in Figure 5 have been aggregated for the sake of exposition. However, our economic model disaggregates each country into 65 sectors allowing us to identify more specifically which economic activities are most vulnerable in West Africa. These more detailed results across 65 sectors are provided in Figure S9 in Supporting Information S1 which further emphasizes the outsized role of agriculture in West Africa's overall labor productivity losses. Raw milk and fishing are the farm and food subsectors contributing most to West Africa's labor capacity losses, but we find that all agricultural subsectors in the region are vulnerable.

Our model also permits analysis of other aspects of economic impacts including changes in global bilateral trade. However, we restrict the focus of this paper on poverty and its drivers. A summary of the trade impacts of the regional impacts of global human heat stress from climate changes is provided in Table S6 in Supporting Information S1. We find that across all seven West African countries, there is a consistent decline in agricultural exports (that exceed declines in overall exports) while agricultural imports are less affected—implying a rise in net food imports (or a decline in net exports).

3.3. Poverty Impacts Across Countries

As described in earlier sections, we assess poverty impacts in seven West African countries using a household microsimulation approach. In six of the seven countries, poverty is increased as a result of heat stress-induced labor capacity losses in our experiments. However, our results suggest that it is possible in some cases that poverty of income sees little change (and in theory can even fall). As detailed below, this is because labor productivity losses can in fact raise the monetary incomes of some households as more labor is needed to maintain agricultural production and higher returns to labor are needed to induce increased employment in agriculture.

The countries that see the largest poverty headcount increases are Ghana and Nigeria where poverty increases by 9.2% and 7.2%, respectively. See Figure 6. The remaining countries (Senegal, Burkina Faso, Cote d'Ivoire, and Cameroon) see poverty increases of 2.3%–5.1%. The exception in our sample is Guinea, where poverty sees little change. As before, these results are based on the ISO-LRF approach. Poverty results are necessarily smaller if the Lancet-LRF is adopted (see Figure S8 in Supporting Information S1) but in this case increases in mortality and morbidities would accompany the poverty increase.

Figure 6 also shows poverty changes at the stratum level (right panel). It reveals that some household types are far more affected by heat stress: Rural diverse and nonagricultural households suffer most. In Nigeria, most of the increase in poverty can be attributed to the rural diverse and the nonagricultural strata. It is these two strata that drive approximately 70% of the country level poverty increase. In contrast, the smallest poverty increases are among households that fall under the agricultural stratum, and in the case of Guinea, poverty in the agricultural stratum actually declines. In the next section, the poverty changes in Nigeria are fully decomposed and this helps highlight the household features and economic mechanisms driving these results.

3.3.1. Drivers of Poverty—Nigeria as a Case Study

To better develop our understanding of how heat stress-induced labor capacity losses drive changes in poverty, we use the case of Nigeria to fully describe how an individual country's poverty impacts are determined.

As described in the methods section, the starting point for determining poverty is the change in consumption prices and wages (returns to factors of production) determined by the global GE model. In Figure 7, changes in consumer prices are compared across the seven countries of focus. It shows that in Nigeria's case, the price of crops increases far more sharply than the other countries. This commodity group accounts for 52% of poor households' spending budget in Nigeria (not shown) and thus the cost of living at the poverty line increases far more sharply. This increase in cost of living acts as a deflator for the "nominal" factor returns/income in Equation 4, pushing down real returns to all factors of production. Changes in real factor returns in Nigeria are summarized in Figure 8, left panel. It shows that real returns to agricultural unskilled labor increase. This is the result of increased demand for this type of labor. The increased demand stems from the fact that labor capacity losses in agriculture and for "blue collar"/unskilled workers are especially high relative to other sectors, with

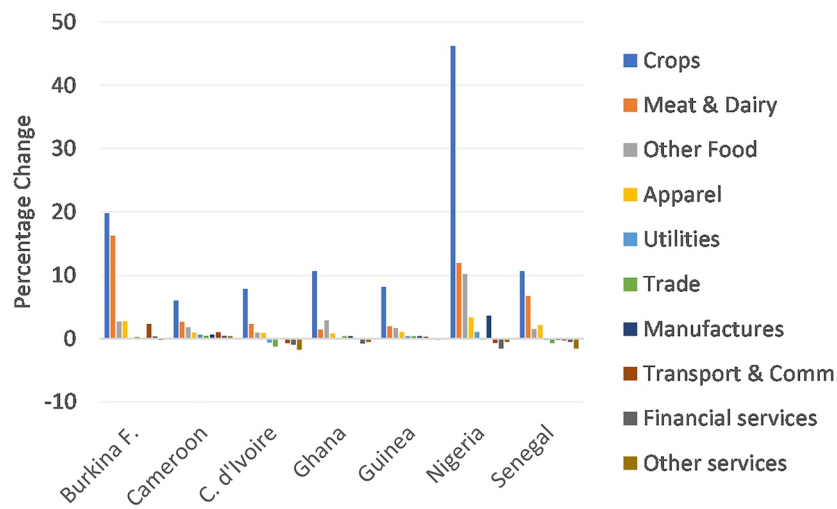

Figure 7. Changes in consumer prices, by commodity group and country.

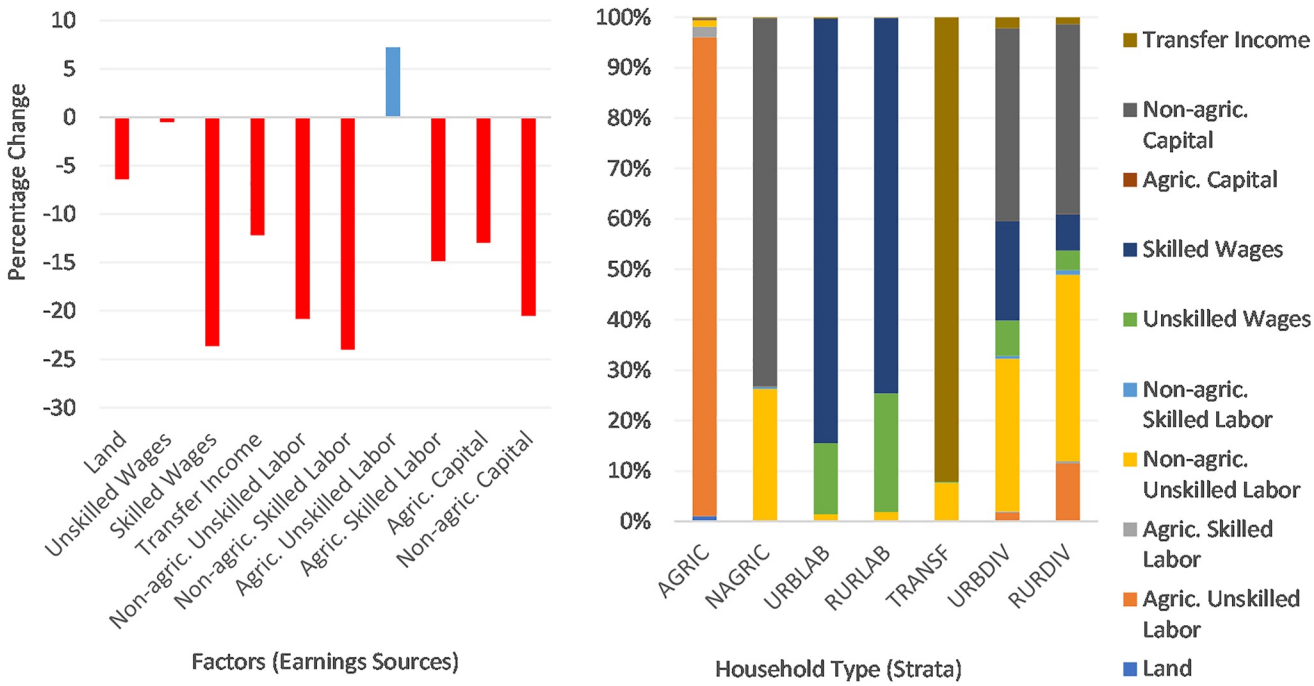

Figure 8. Real returns to factors (left panel) and factor earning shares by household stratum (right panel) in Nigeria.

labor capacity losses acting as a reduction in effective labor supply and hence income. Furthermore, given that agricultural production is a necessity, as each unit of labor becomes less productive, more must be drawn into the sector to dampen output losses necessitating higher returns for agricultural labor. This increase in returns to unskilled agricultural labor therefore also occurs in other countries (not shown).

These wage and price changes determine changes in real incomes of the seven household types, taking into account their earning shares (see Equation 4 in the methods section). This approach accounts for the fact that changes in wages of skilled labor play a larger role for households that earn most of their income from skilled wage employment and less of a role for households that earn most of their income from agricultural self-employment. Figure 8b shows the earning shares of households near the poverty line in Nigeria. We see that the agricultural stratum earns most of its income from unskilled labor; the factor that sees its returns increase. This explains why the agricultural stratum tends to show improvements in poverty in our results: Incomes for households in this stratum rise as they earn a large portion of their income from agricultural unskilled labor; the factor of production that experiences increasing returns. In contrast, the rural diverse stratum in Nigeria earns a significant portion of its income from capital, returns to which can be seen in Panel A to be declining by much larger margins than the increase in returns to agricultural labor.

As a result, in Nigeria, all households near the poverty line, except those that fall under the agricultural stratum, see large decreases in real income. Figure 9 shows the decline in real incomes by stratum in Nigeria as well as the other six West African economies considered in the poverty analysis. It is these changes in income that we utilize in the household microsimulation. We then determine how many households fall into (and out of) poverty as a result. The income changes shown in Figure 9 explain in large part the patterns of poverty changes reported in Figure 6: The large increases in poverty in Nigeria.

4. Discussion

In this study, we have assessed the potential poverty consequences of heat stress-induced labor capacity losses, with a focus toward determining the economic channels and factors that determine these poverty outcomes. We therefore assess poverty at the level of earning sources-based household strata. This undertaking inevitably presents a number of uncertainties including the following: Uncertainties in the estimation and projections of heat stress itself, labor capacity losses associated with heat stress—for which there are a variety of alternative

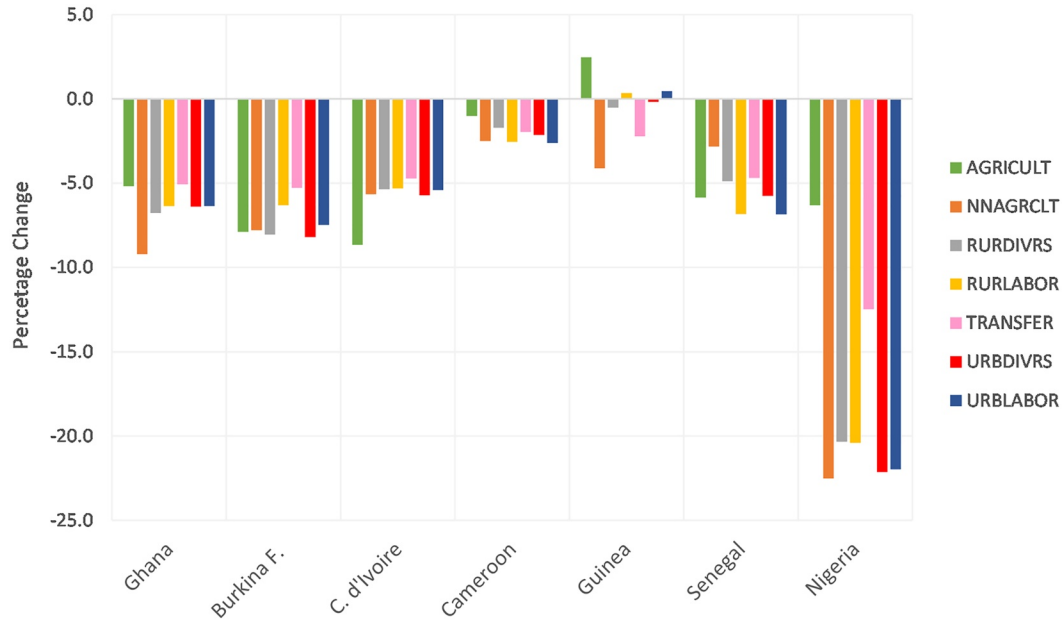

Figure 9. Real incomes near the poverty line by household stratum and country.

methodologies, there is limited data regarding work intensities and outdoor exposure rates of workers across the globe, and the economic model employs critical assumptions that will affect estimated results. Given the prominence of wage changes associated with the projected losses in labor capacity, the assumptions regarding the mobility of labor across sectors, and how global economic structures and the distribution and composition of poverty will evolve over time, are all important considerations when assessing the robustness of the findings provided here.

As described at length under the methods section, uncertainties surrounding the estimation of heat stress have been carefully addressed for this study using more accurate estimates of the WBGT, based on the latest methods (Kong & Huber, 2022). However, there remains considerable uncertainty about how these changes in WBGT will affect labor capacities across labor types and sectors. To address this issue, we considered an alternative labor response function to estimate labor capacity losses. Implicit in our primary labor capacity calculations and the results reported above is the assumption that ISO standards for shaded rest are followed. In practice, workers may adjust their work pace when exposed to high levels of heat and humidity without referring to any standards, some workers may tend to overwork under heat. Using an alternative assessment of labor capacity losses based on an empirically determined labor response function (Romanello et al., 2021; Watts et al., 2021), the magnitudes of immediate labor capacity changes are necessarily smaller: Poverty increases by 6.4% in Nigeria followed by Ghana and Senegal where poverty increases by 3.2%–3.3% (see Figure S8 in Supporting Information S1). However, if the ISO guidelines are not followed, then the increases in poverty would coincide with increases in worker mortality and morbidities that remain unaccounted. Future work should include health and mortality costs associated with labor outcome.

Additional uncertainties associated with labor capacity changes are associated with alternative assumptions regarding outdoor exposure rates of workers across the globe as well as alternative assumptions regarding labor mobility across sectors. Here, we have relied on empirical evidence from just a few countries. However, these characteristics are likely to vary greatly across regions and income levels. However, sensitivity analysis presented in the supplementary materials (Texts S2 and S3 in Supporting Information S1) show that alternative assumptions about these factors do not affect results as substantially.

Another important limitation of this study is the reliance on a comparative static, global static, and GE model to assess the impacts of a future climate scenario (one of 3°C mean global warming) on the present-day economy. This comparative static approach allows us to clearly identify the mechanisms that drive our results with relative clarity and avoids the tremendous uncertainties involved in projecting the composition and distribution of poverty

and economic structures in the distant future. Indeed, the precise date at which 3°C mean global warming might come to pass is itself quite uncertain, leaving further challenges for economic models seeking for forecast future poverty outcomes. These challenges, together with the capability to readily identify the economic mechanisms driving poverty changes, provide the rationale for the comparative static approach presented in this paper.

Based on this approach, at the national level, most countries considered in our poverty analysis see poverty levels increase. While we allow for some forms of adaptation, the GTAP model allows for greater mechanization (i.e., capital-labor substitution in the face of diminished labor productivity), movement of labor across sectors, and changes in consumption patterns, these are insufficient to prevent significant output reductions in key sectors. We acknowledge, however, that there are many other adaptation options for workers including shifting to night work (Takakura et al., 2018) and various others (Day et al., 2019), not accounted for in our results. The resulting GDP and output losses are most pronounced in West Africa due to its dependence on agriculture and the prevalence of highly exposed, low-skilled labor employed in this sector. In our sample of seven West African countries, Ghana and Nigeria are most concerning as we see large percentage increases in poverty of 11.7% and 10% respectively. Other countries in our sample see poverty increases ranging between 3.7% and 5.6%. The exception is Guinea which experiences little change in poverty.

Focusing on Nigeria, one of the most populous countries in the world, we fully decompose the underlying drivers of poverty. Nigeria's poverty outcome is driven by a sharp rise in food prices and a strong increase in the real cost of living at the poverty line. This is further exacerbated by a large concentration of households just above the poverty line. More generally, we find that the impact of labor productivity losses on relative factor returns is a key mechanism that determines the direction and magnitude of poverty headcount changes. Hourly wage rates for unskilled agricultural labor can increase as more labor must be drawn into agriculture to maintain food production. However, households are able to work fewer hours under these new conditions. Rising wage costs result in lower returns to other factors of production and so households that are diversified and rely on land, capital, and nonfarm wages are most adversely affected in our experiments. In conclusion, how households at the poverty line earn their income is key in determining the extent to which a country's poverty headcount will be affected by heat stress-induced losses in labor capacity under a warming climate.

Data Availability Statement

Coupled Model Intercomparison Project Phase 6 (CMIP6) data set can be retrieved from the open-source link, https://esgf-node.llnl.gov/search/cmip6/. Users should select the models (source ID) and variant label as indicated in Table S4 in Supporting Information S1, the frequency as 3 hourly (3 hr), and the experiment ID as either historical or ssp585. Variables needed include 2m temperature (tas), specific humidity (huss), 10m wind speed (uas and vas), surface downwelling shortwave flux (rsds), surface upwelling shortwave flux (rsus), surface downwelling longwave flux (rlds), and surface upwelling longwave flux (rlus). Data can be downloaded as NetCDF files that appear in the search outputs. ERA5 reanalysis data were downloaded from the Copernicus Climate Change Service (C3S) Climate Data Store (https://cds.climate.copernicus.eu/cdsapp#!/dataset/reanalysis-era5-single-levels?tab=form). The results contain modified Copernicus Climate Change Service information 2020. Neither the European Commission nor ECMWF is responsible for any use that may be made of the Copernicus information or data it contains. The WBGT calculation code along with a Jupyter notebook introducing its usage is deposited in Zenodo (https://zenodo.org/record/5980536). The BLS Occupational Requirement Survey data for 2021 are available at https://www.bls.gov/ors/data.htm. Household survey data sets for the seven West African countries can be obtained as follows. Ghana: https://www2.statsghana.gov.gh/nada/index.php/catalog/97; Burkina Faso: https://microdata.worldbank.org/index.php/catalog/2538; Cameroon: http://slmp-550-104.slc.westdc.net/~stat54/nada/index.php/catalog/114; Cote d' Ivoire: http://catalog.ihsn.org/catalog/7330; Guinea: https://catalog.ihsn.org/catalog/5122; Nigeria: https://microdata.worldbank.org/index.php/catalog/3557; and Senegal: https://catalog.ihsn.org/catalog/4311. GTAP simulation results can be reproduced using the GTAP archive provided at https://www.gtap.agecon.purdue.edu/resources/res_display.asp?RecordID=6478. The archive contains the model code, data, and experiment files. A GTAP database license is required for access to data and a GEMPACK license is required to reproduce results using the runGTAP software available at https://www.gtap.agecon.purdue.edu/products/rungtap/default.asp. Stata do files for processing the household survey data and reproducing poverty results using household microsimulations are also provided at https://www.gtap.agecon.purdue.edu/resources/res_display.asp?RecordID=6478. Analyses of CMIP data were performed

on Purdue University's high-performance computing cluster using Python (Van Rossum & Drake, 2009) and CDO (Schulzweida, 2019). The following Python packages were utilized: Numpy (Harris et al., 2020), Scipy (Virtanen et al., 2020), Xarray (Hoyer & Hamman, 2017), Dask (Dask Development Team, 2016), Matplotlib (Hunter, 2007), and Cartopy (Met Office, 2010–2015). The gridded data analysis for labor type and economic sectors is done in R (R Core Team, 2021) using the following packages: terra (v1.5-21, Hijmans et al., 2022), raster (v3.5-11, Hijmans et al., 2021), and reshape2 (v 1.4.4, Wickham, 2020).

Acknowledgments
MH and TH acknowledge funding from NSF-OISE-2020635. TH also acknowledges funding from NSF-CBET 1855937 and USDA Hatch 1003642. SC thanks Nithya Srinivasan and Yeqing Qu for their excellent research assistance.

References

ABM. (2010). About the approximation to the WBGT used by the Bureau of Meteorology. Retrieved from http://www.bom.gov.au/info/thermal_stress/#approximation

Aguiar, A., Chepeliev, M., Corong, E. L., McDougall, R., & Van Der Mensbrugghe, D. (2019). The GTAP data base: Version 10. *Journal of Global Economic Analysis*, *4*(1), 1–27. https://doi.org/10.21642/JGEA.040101AF

Alizadeh, M. R., Abatzoglou, J. T., Adamowski, J. F., Prestemon, J. P., Chittoori, B., Akbari Asanjan, A., & Sadegh, M. (2022). Increasing heat-stress inequality in a warming climate. *Earth's Future*, *10*(2), e2021EF002488. https://doi.org/10.1029/2021ef002488

Altinsoy, H., & Yildirim, H. A. (2015). Labor productivity losses over western Turkey in the twenty-first century as a result of alteration in WBGT. *International Journal of Biometeorology*, *59*(4), 463–471. https://doi.org/10.1007/s00484-014-0863-z

American College of Sports Medicine. (1984). Prevention of thermal injuries during distance running. *Medicine & Science in Sports & Exercise*, *16*, iv–xiv.

ANSD. (2011). *Poverty Monitoring Survey in Senegal 2011, (original title: Enquête de Suivi de la Pauvreté au Sénégal 2011). Agence Nationale de la Statistique et de la Démographie Ministère de l'Economie et des Finances (MEF)*. International Household Survey Network. Reference ID: SEN_2011_ESPS-II_v01_M. Retrieved from https://catalog.ihsn.org/catalog/4311

Baldos, U. L. C. (2017). *Development of GTAP version 9 land use and land cover database for years 2004, 2007 and 2011 (No. 5424)*. Center for Global Trade Analysis, Department of Agricultural Economics, Purdue University.

Baldos, U. L. C., Haqiqi, I., Hertel, T. W., Horridge, M., & Liu, J. (2020). SIMPLE-G: A multiscale framework for integration of economic and biophysical determinants of sustainability. *Environmental Modelling & Software*, *133*, 104805. https://doi.org/10.1016/j.envsoft.2020.104805

BLS. (2020). *The occupational Requirements survey (ORS)*. Bureau of Labor Statistics. (BLS).

Bröde, P., Fiala, D., Lemke, B., & Kjellstrom, T. (2018). Estimated work ability in warm outdoor environments depends on the chosen heat stress assessment metric. *International Journal of Biometeorology*, *62*(3), 331–345. https://doi.org/10.1007/s00484-017-1346-9

Buzan, J. R., & Huber, M. (2020). Moist heat stress on a hotter Earth. *Annual Review of Earth and Planetary Sciences*, *48*(1), 623–655. https://doi.org/10.1146/annurev-earth-053018-060100

Casanueva, A., Kotlarski, S., Fischer, A. M., Flouris, A. D., Kjellstrom, T., Lemke, B., et al. (2020). Escalating environmental summer heat exposure—A future threat for the European workforce. *Regional Environmental Change*, *20*(2), 1–14. https://doi.org/10.1007/s10113-020-01625-6

Chavaillaz, Y., Roy, P., Partanen, A.-I., Da Silva, L., Bresson, É., Mengis, N., et al. (2019). Exposure to excessive heat and impacts on labour productivity linked to cumulative CO_2 emissions. *Scientific Reports*, *9*(1), 13711. https://doi.org/10.1038/s41598-019-50047-w

CIESIN (2018). *Gridded population of the world, version 4 (GPWv4): Administrative unit center points with population estimates, Revision 11*. Center for International Earth Science Information Network–CIESIN–Columbia University, NASA Socioeconomic Data and Applications Center (SEDAC).

Coco, A., Jacklitsch, B., Williams, J., Kim, J. H., Musolin, K., & Turner, N. (2016). *Criteria for a recommended standard: Occupational exposure to heat and hot environments*. Department of Health and Human Services, Centers for Disease Control and Prevention, National Institute for Occupational Safety and Health. Retrieved from https://www.elcosh.org/record/document/3998/d001392.pdf

Corong, E. L., Hertel, T. W., McDougall, R., Tsigas, M. E., & van der Mensbrugghe, D. (2017). The standard GTAP model, version 7. *Journal of Global Economic Analysis*, *2*(1), 1–119. https://doi.org/10.21642/JGEA.020101AF

Day, E., Fankhauser, S., Kingsmill, N., Costa, H., & Mavrogianni, A. (2019). Upholding labour productivity under climate change: An assessment of adaptation options. *Climate Policy*, *19*(3), 367–385. https://doi.org/10.1080/14693062.2018.1517640

de Lima, C. Z., Buzan, J. R., Moore, F. C., Baldos, U. L. C., Huber, M., & Hertel, T. W. (2021). Heat stress on agricultural workers exacerbates crop impacts of climate change. *Environmental Research Letters*, *16*(4), 044020. https://doi.org/10.1088/1748-9326/abeb9f

Dunne, J. P., Stouffer, R. J., & John, J. G. (2013). Reductions in labour capacity from heat stress under climate warming. *Nature Climate Change*, *3*(6), 563–566. https://doi.org/10.1038/nclimate1827

FAO. (2020). Producer prices, food and agricultural organization of the united Nations. Retrieved from https://www.fao.org/faostat/en/#data/PP%20on%2010/31/2020

Ferreira, F. H., Chen, S., Dabalen, A., Dikhanov, Y., Hamadeh, N., Jolliffe, D., et al. (2016). A global count of the extreme poor in 2012: Data issues, methodology and initial results. *The Journal of Economic Inequality*, *14*(2), 141–172. https://doi.org/10.1007/s10888-016-9326-6

Flouris, A. D., Dinas, P. C., Ioannou, L. G., Nybo, L., Havenith, G., Kenny, G. P., & Kjellstrom, T. (2018). Workers' health and productivity under occupational heat strain: A systematic review and meta-analysis. *The Lancet Planetary Health*, *2*(12), e521–e531. https://doi.org/10.1016/s2542-5196(18)30237-7

Foster, J., Smallcombe, J. W., Hodder, S., Jay, O., Flouris, A. D., Nybo, L., & Havenith, G. (2021). An advanced empirical model for quantifying the impact of heat and climate change on human physical work capacity. *International Journal of Biometeorology*, *65*(7), 1215–1229. https://doi.org/10.1007/s00484-021-02105-0

Grundstein, A., & Cooper, E. (2018). Assessment of the Australian Bureau of Meteorology wet bulb globe temperature model using weather station data. *International Journal of Biometeorology*, *62*(12), 2205–2213. https://doi.org/10.1007/s00484-018-1624-1

GSS. (2018). Ghana living standard survey (GLSS 7) 2017. Ghana statistical service (GSS), national data archive. (NADA), ID number: DDI-GHA-GSS-GLSS7-2017-v1. Retrieved from https://www2.statsghana.gov.gh/nada/index.php/catalog/97

Haqiqi, I., Grogan, D. S., Horeh, M. B., Liu, J., Baldos, U. L. C., & Hertel, T. (2020). Environmental stressors can intensify the impacts of pandemics on Earth's natural resources and global food systems. *AGU Fall Meeting Abstracts*, *2020*, GH023–05.

Harris, C. R., Millman, K. J., van der Walt, S. J., Gommers, R., Virtanen, P., Cournapeau, D., et al. (2020). Array programming with NumPy. *Nature*, *585*(7825), 357–362. https://doi.org/10.1038/s41586-020-2649-2

Havenith, G., & Fiala, D. (2011). Thermal indices and thermophysiological modeling for heat stress. *Comprehensive Physiology*, *6*(1), 255–302. https://doi.org/10.1002/cphy.c140051

Hersbach, H., Bell, B., Berrisford, P., Biavati, G., Horányi, A., Muñoz Sabater, J., et al. (2018). ERA5 hourly data on single levels from 1979 to present. *Copernicus Climate Change Service (C3S) Climate Data Store (CDS)*, *10*.

Hertel, T., Verma, M., Ivanic, M., Magalhaes, E., Ludena, C., & Rios, A. R. (2011). GTAP-POV: A framework for assessing the national poverty impacts of global economic and environmental policies. Retrieved from https://www.gtap.agecon.purdue.edu/resources/res_display.asp?RecordID=3731

Hertel, T. W. (1997). *Global trade analysis: Modeling and applications*. Cambridge university press.

Hertel, T. W., Burke, M. B., & Lobell, D. B. (2010). The poverty implications of climate-induced crop yield changes by 2030. *Global Environmental Change*, *20*(4), 577–585. https://doi.org/10.1016/j.gloenvcha.2010.07.001

Hijmans, R. J., Bivand, R., Forner, K., Ooms, J., Pebesma, E., & Sumner, M. D. (2022). 'Terra': Spatial data analysis, R package. https://CRAN.R-project.org/package=terra

Hijmans, R. J., Van Etten, J., Cheng, J., Mattiuzzi, M., Sumner, M., Greenberg, J. A., et al. (2021). 'Raster': Geographic data analysis and modeling. R package. Retrieved from https://CRAN.R-project.org/package=raster

Hoyer, S., & Hamman, J. (2017). xarray: N-D labeled Arrays and Datasets in Python. *Journal of Open Research Software*, *5*(1), 10. https://doi.org/10.5334/jors.148

Hunter, J. D. (2007). Matplotlib: A 2D graphics environment. *Computing in Science & Engineering*, *9*(3), 90–95. https://doi.org/10.1109/MCSE.2007.55

ILO. (2019). *Working on A warming Planet: The impact of heat stress on labour productivity and decent work*. ILO.

INS. (2017). *The Fourth Cameroon Household Survey, (original title: Quatrième Enquête Camerounaise Auprès des Ménages)*. Institut National de la Statistique. (INS), Ministère de l'Economie, de la Planification et de l'Aménagement du Territoire, Enquêtes Camerounaises Auprès des Ménages, ID: CMR-INS-ECAM4-V1.2. Retrieved from http://slmp-550-104.slc.westdc.net/~stat54/nada/index.php/catalog/114

INS-CI. (2015). Household Standard of Living Survey 2015, (original title: Enquête sur le Niveau de Vie des Ménages 2015). Reference ID: CIV_2015_ENV_v01_M. In *Institut National de la Statistique, Ministère du Plan et du Développement, Côte d'Ivoire*. International Household Survey Network. Retrieved from http://catalog.ihsn.org/catalog/7330

INSD. (2014). Continuous multisectoral survey 2014, (original title: Enquête Multisectorielle Continue 2014). In *Institut National de la Statistique et de la Démographie (INDS), Ministère de l'Economie et des Finances, Burkina Faso*. The World Bank Microdata Library, Living Standards Measurement Study, Reference ID: BFA_2014_EMC_v01_M. Retrieved from https://microdata.worldbank.org/index.php/catalog/2538

INS-Guinée. (2012). Poverty assessment survey 2012, (original title: Enquête légère pour l'Evaluation de la Pauvreté 2012). In *Institut National de la Statistique*. International Household Survey Network, Reference ID: GIN_2012_ELEP_v01_M. Retrieved from https://catalog.ihsn.org/catalog/5122

International Organization for Standardization (ISO). (2017). Hot environments—Ergonomics of the Thermal environment—Assessment of heat stress using the WBGT (Wet Bulb globe temperature) index. ISO Standard 7243.

Ioannou, L. G., Foster, J., Morris, N. B., Piil, J. F., Havenith, G., Mekjavic, I. B., et al. (2022). Occupational heat strain in outdoor workers: A comprehensive review and meta-analysis, (pp. 1–36).

Keeney, R., & Hertel, T. (2005). GTAP-AGR: A framework for assessing the implications of multilateral changes in agricultural policies. GTAP Technical Papers (Vol. *25*). Retrieved from https://www.gtap.agecon.purdue.edu/resources/res_display.asp?RecordID=1869

Kjellstrom, T., Briggs, D., Freyberg, C., Lemke, B., Otto, M., & Hyatt, O. (2016). Heat, human performance, and occupational health: A key issue for the assessment of global climate change impacts. *Annual Review of Public Health*, *37*(1), 97–112. https://doi.org/10.1146/annurev-publhealth-032315-021740

Kjellstrom, T., Freyberg, C., Lemke, B., Otto, M., & Briggs, D. (2018). Estimating population heat exposure and impacts on working people in conjunction with climate change. *International Journal of Biometeorology*, *62*(3), 291–306. https://doi.org/10.1007/s00484-017-1407-0

Kjellstrom, T., Kovats, R. S., Lloyd, S. J., Holt, T., & Tol, R. S. (2009). The direct impact of climate change on regional labor productivity. *Archives of Environmental & Occupational Health*, *64*(4), 217–227. https://doi.org/10.1080/19338240903352776

Knittel, N., Jury, M. W., Bednar-Friedl, B., Bachner, G., & Steiner, A. K. (2020). A global analysis of heat-related labour productivity losses under climate change—Implications for Germany's foreign trade. *Climatic Change*, *160*(2), 251–269. https://doi.org/10.1007/s10584-020-02661-1

Kong, Q., & Huber, M. (2022). Explicit Calculations of Wet-Bulb Globe Temperature Compared With Approximations and Why It Matters for Labor Productivity. *Earth's Future*, *10*(3). https://doi.org/10.1029/2021ef002334

Lee, S.-M., & Min, S.-K. (2018). Heat stress changes over East Asia under 1.5° and 2.0°C global warming targets. *Journal of Climate*, *31*(7), 2819–2831. https://doi.org/10.1175/JCLI-D-17-0449.1

Liljegren, J. C., Carhart, R. A., Lawday, P., Tschopp, S., & Sharp, R. (2008). Modeling the wet bulb globe temperature using standard meteorological measurements. *Journal of Occupational and Environmental Hygiene*, *5*(10), 645–655. https://doi.org/10.1080/15459620802310770

Liu, X. (2020). Reductions in labor capacity from intensified heat stress in China under future climate change. *International Journal of Environmental Research and Public Health*, *17*(4), 1278. https://doi.org/10.3390/ijerph17041278

Matsumoto, K., Tachiiri, K., & Su, X. (2021). Heat stress, labor productivity, and economic impacts: Analysis of climate change impacts using two-way coupled modeling. *Environmental Research Communications*, *3*(12), 125001. https://doi.org/10.1088/2515-7620/ac3e14

Met Office. (2010–2015). Cartopy: A cartographic python library with a matplotlib interface [computer software manual]. Exeter. Retrieved from https://scitools.org.uk/cartopy

Moore, F. C., Lacasse, K., Mach, K. J., Shin, Y. A., Gross, L. J., & Beckage, B. (2022). Determinants of emissions pathways in the coupled climate–social system. *Nature*, *603*(7899), 103–111. https://doi.org/10.1038/s41586-022-04423-8

Moran, D. S., Pandolf, K. B., Laor, A., Heled, Y., Matthew, W. T., & Gonzalez, R. R. (2003). Evaluation and refinement of the environmental stress index for different climatic conditions. *Journal of Basic and Clinical Physiology and Pharmacology*, *14*(1), 1–16. https://doi.org/10.1515/JBCPP.2003.14.1.1

Moran, D. S., Pandolf, K. B., Shapiro, Y., Heled, Y., Shani, Y., Mathew, W. T., & Gonzalez, R. R. (2001). An environmental stress index (ESI) as a substitute for the wet bulb globe temperature (WBGT). *Journal of Thermal Biology*, *26*(4–5), 427–431. https://doi.org/10.1016/S0306-4565(01)00055-9

NBS. (2018). General household survey, panel 2018–2019, wave 4. *The World Bank Microdata Library, Living Standards Measurement Study*, Reference ID: NGA_2018_GHSP-W4_v03_M, National Bureau of Statistics (NBS), Federal Government of Nigeria. Retrieved from https://microdata.worldbank.org/index.php/catalog/3557

Orlov, A., Sillmann, J., Aunan, K., Kjellstrom, T., & Aaheim, A. (2020). Economic costs of heat-induced reductions in worker productivity due to global warming. *Global Environmental Change*, *63*, 102087. https://doi.org/10.1016/j.gloenvcha.2020.102087

Parsons, L. A., Masuda, Y. J., Kroeger, T., Shindell, D., Wolff, N. H., & Spector, J. T. (2022). Global labor loss due to humid heat exposure underestimated for outdoor workers. *Environmental Research Letters*, *17*(1), 014050. https://doi.org/10.1088/1748-9326/ac3dae

Parsons, L. A., Shindell, D., Tigchelaar, M., Zhang, Y., & Spector, J. T. (2021). Increased labor losses and decreased adaptation potential in a warmer world. *Nature Communications*, *12*(1), 7286. https://doi.org/10.1038/s41467-021-27328-y

Rogers, C. D. W., Ting, M., Li, C., Kornhuber, K., Coffel, E. D., Horton, R. M., et al. (2021). Recent increases in exposure to extreme humid-heat events disproportionately affect populated regions. *Geophysical Research Letters*, *48*(19), e2021GL094183. https://doi.org/10.1029/2021gl094183

Romanello, M., McGushin, A., Di Napoli, C., Drummond, P., Hughes, N., Jamart, L., et al. (2021). The 2021 report of the Lancet Countdown on health and climate change: Code red for a healthy future. *The Lancet*, *398*(10311), 1619–1662. https://doi.org/10.1016/S0140-6736(21)01787-6

Sahu, S., Sett, M., & Kjellstrom, T. (2013). Heat exposure, cardiovascular stress and work productivity in rice harvesters in India: Implications for a climate change future. *Industrial Health*, *51*(4), 424–431. https://doi.org/10.2486/indhealth.2013-0006

Sawka, M. N., Wenger, C. B., Montain, S. J., Kolka, M. A., Bettencourt, B., Flinn, S., et al. (2003). *Heat stress control and heat casualty management*. Army Research Inst of Environmental Medicine Natick Ma. Retrieved from https://apps.dtic.mil/sti/citations/ADA433236

Schulzweida, U. (2019). Cdo user guide. https://doi.org/10.5281/zenodo.3539275

Schwingshackl, C., Sillmann, J., Vicedo-Cabrera, A. M., Sandstad, M., & Aunan, K. (2021). Heat stress indicators in CMIP6: Estimating future trends and exceedances of impact-relevant thresholds. *Earth's Future*, *9*(3), e2020EF001885. https://doi.org/10.1029/2020ef001885

Siebert, S., & Döll, P. (2010). Quantifying blue and green virtual water contents in global crop production as well as potential production losses without irrigation. *Journal of Hydrology*, *384*(3–4), 198–217. https://doi.org/10.1016/j.jhydrol.2009.07.031

Takakura, J., Fujimori, S., Takahashi, K., Hasegawa, T., Honda, Y., Hanasaki, N., et al. (2018). Limited role of working time shift in offsetting the increasing occupational-health cost of heat exposure. *Earth's Future*, *6*(11), 1588–1602. https://doi.org/10.1029/2018EF000883

Takakura, J. Y., Fujimori, S., Takahashi, K., Hijioka, Y., Hasegawa, T., Honda, Y., & Masui, T. (2017). Cost of preventing workplace heat-related illness through worker breaks and the benefit of climate-change mitigation. *Environmental Research Letters*, *12*(6), 064010. https://doi.org/10.1088/1748-9326/aa72cc

Van Rossum, G., & Drake, F. L. (2009). Python 3 reference manual, CreateSpace.

Virtanen, P., Gommers, R., Oliphant, T. E., Haberland, M., Reddy, T., Cournapeau, D., et al. (2020). SciPy 1.0: Fundamental algorithms for scientific computing in Python. *Nature Methods*, *17*(3), 261–272. https://doi.org/10.1038/s41592-019-0686-2

Watts, N., Amann, M., Arnell, N., Ayeb-Karlsson, S., Beagley, J., Belesova, K., et al. (2021). The 2020 report of the Lancet Countdown on health and climate change: Responding to converging crises. *The Lancet*, *397*(10269), 129–170. https://doi.org/10.1016/S0140-6736(20)32290-X

Wickham (2020). 'Reshape2': Flexibly reshape data: A reboot of the reshape package, R package. Retrieved from https://CRAN.R-project.org/package=reshape2

Wyndham, C. H. (1969). Adaptation to heat and cold. *Environmental Research*, *2*(5–6), 442–469. https://doi.org/10.1016/0013-9351(69)90015-2

Zhang, Y., & Shindell, D. T. (2021). Costs from labor losses due to extreme heat in the USA attributable to climate change. *Climatic Change*, *164*(3–4), 35. https://doi.org/10.1007/s10584-021-03014-2

Zhu, J., Wang, S., Zhang, B., & Wang, D. (2021). Adapting to changing labor productivity as a result of intensified heat stress in a changing climate. *GeoHealth*, *5*(4). https://doi.org/10.1029/2020GH000313